



You have downloaded a document from
RE-BUŚ
repository of the University of Silesia in Katowice

Title: Dendritic structure analysis of CMSX-4 cored turbine blades roots

Author: Jacek Krawczyk

Citation style: Krawczyk Jacek. (2016). Dendritic structure analysis of CMSX-4 cored turbine blades roots. "Archives of Metallurgy and Materials" (2016, vol. 61 iss. 2B, s. 1129-1134), doi 10.1515/amm-2016-0189



Uznanie autorstwa - Użycie niekomercyjne - Bez utworów zależnych Polska - Licencja ta zezwala na rozpowszechnianie, przedstawianie i wykonywanie utworu jedynie w celach niekomercyjnych oraz pod warunkiem zachowania go w oryginalnej postaci (nie tworzenia utworów zależnych).



UNIwersYTET ŚLĄSKI
W KATOWICACH



Biblioteka
Uniwersytetu Śląskiego



Ministerstwo Nauki
i Szkolnictwa Wyższego

DENDRITIC STRUCTURE ANALYSIS OF CMSX-4 CORED TURBINE BLADES ROOTS

The microstructure of *as-cast* cored turbine blades roots, made of the single-crystal CMSX-4 nickel-based superalloy was investigated. Analysed blades were obtained by directional solidification technique in the industrial ALD Bridgman induction furnace. The investigations of the microstructure of blades roots were performed using SEM and X-ray techniques including diffraction topography with the use of Auleytner method. Characteristic shapes of dendrites with various arrangement were observed on the SEM images taken from the cross-sections, made transversely to the main blades axis. The differences in quality of the structure in particular areas of blades roots were revealed. Based on the results, the influence of cooling bores on blades root structure was analysed and the changes in the distribution and geometry of cooling bores were proposed.

Keywords: single-crystalline turbine blades, nickel-base superalloy, dendritic structure, X-ray topography, SEM

1. Introduction

Nowadays, the single-crystalline structural materials are frequently used in many high-tech industry sectors. Nickel, cobalt or iron-based alloys form a group of materials, which are used, *inter alia*, for the production of structural components in gas turbines or aircraft engines. These high-temperature alloys exhibit a high creep resistance and heat resistance while retaining high mechanical strength. Single-crystalline nickel-based alloys, also known as superalloys, belong to this group of materials. Superalloys are a group of materials which, through their specific properties are used, among others, in the production of blades for gas turbines and aircraft engines. The conditions, in which the blades work, require specific strength properties, that are met by an industrial nickel-based superalloy – the CMSX-4. It is resistant to prolonged exposure at high temperatures and has a high creep resistance, even at elevated temperatures under the heavy loads of multiaxial stresses acting during the operation of blades [1-3].

The blades working conditions and environment in the engine turbine, determine, *inter alia*, their construction and method of protection against high temperatures. The making of the cooling bores, that improve heat dissipation, is one of methods to protect the material of blades. Despite good mechanical properties and durability, structural studies of nickel-based superalloys are continued. The aim of these studies is to optimize the casting technology and arrangement of cooling bores, leading to the improvement to the operating temperature capability, fatigue strength, corrosion resistance and creep

resistance. Another important stage in the development of superalloys comprises studies on the influence of destructive mechanisms occurring during the operation on the structural perfection and the increasing of the turbine components reliability [4-5]. The term structural perfection describes the deviation from the ideal geometry of structure, for example regularity in dendrites distribution and the size of dendrite arms (structure quality), the presence of structural defects (e.g. low angle boundaries) etc.

The crystallographic orientation and structural perfection, associated with the dendritic structure, affect the strength parameters of the turbine blades. These features of the structure of single-crystalline superalloys are directly related to technological parameters of directional solidification by the Bridgman technique and the geometry of obtained components. The geometry of turbine blades of aircraft engines is highly complex (Fig. 1) and affects the deviation from the required structure quality [6]. The cooling bores in the blades cause an increase in the geometry complexity, which may lead to the generation of disorder in the crystal structure (deviation from the preferred crystallographic direction) and even to the creation of defects, e.g. in the form of subgrains or low angle boundaries. The structural perfection reduces also the dendritic cores rotation and the dendrite's arm rotation around its axis [6-8].

The aim of the studies presented in this paper was to analyse the microstructure of the root part of *as-cast* single-crystalline cored turbine blades, made of CMSX-4 nickel-based superalloy and to determine the impact of cooling bores on the blade roots dendritic structure.

* UNIVERSITY OF SILESIA, INSTITUTE OF MATERIALS SCIENCE, 1A 75 PUŁKU PIECHOTY STR., 41-500 CHORZÓW, POLAND

Corresponding author: jacek.krawczyk@us.edu.pl

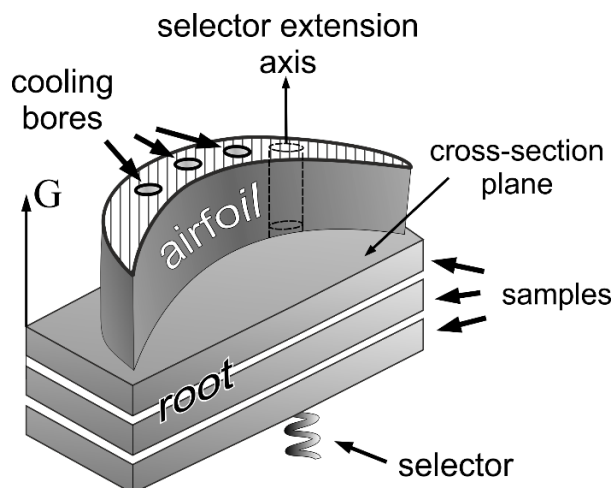


Fig. 1. The shape of the cored turbine blade fragment with a scheme of the sample cutting method. G – the main axis of the blade

2. Experimental

The analysed blades were made of the single-crystal CMSX-4 nickel-based superalloy. The blades were obtained by the directional solidification using the Bridgman technique in an industrial ALD induction furnace. The CMSX-4 nickel-base superalloy consists mainly of two phases: γ – solid solution forming the matrix and γ' – $\text{Ni}_3(\text{Ti,Al})$ based intermetallic phase, which occurs in reinforcement. The microstructure of the single-crystalline CMSX-4 superalloy is characterized by the lack of grain boundaries, even though it is formed by more than one phase [9], due to closely related crystallographic parameters of the two component phases. Both main phases belong to a cubic crystal system, the γ phase has a face-centred crystal (fcc) lattice and the γ' phase has a simple cubic lattice (an ordered type of structure with a derivative of an fcc unit-cell). The lattice parameters of both phases differ by 0.02 \AA [9]. The dendrites existing in the structure of CMSX-4 superalloy are formed mainly by the γ and γ' phases [10,11]. Because of the optimal strength properties of CMSX-4 superalloy, which are shown in the [001] crystallographic direction, the blades (and the dendrite cores at the same time) are produced with the main axis (G – Fig. 1) parallel to the above preferred orientation. Any deviations from this specified direction decrease the quality of blades, therefore the structural perfection plays an important role in their production.

Samples for tests were prepared by cutting off fragments of the blades root (Fig. 2) transversely to the main axis of the blades, at distances of about 5 mm. The metallographic sections were prepared along the cutting planes.

The crystallographic orientation and lattice symmetry in several points on the microsection surface were analysed by



Fig. 2. Photography of an analyzed sample example

the back-reflection Laue method. The X-ray Co radiation was applied. In this method a white incident beam was focused on a stationary single crystalline sample. The selected wavelength ranges of used X-rays were fulfilling the Bragg's law for different types of planes. The diffracted beam is recorded in the X-ray film and creates Laue spots [12].

Dendritic structure observations were performed by a scanning electron microscope (SEM) using the backscattered electron (BSE) technique. The magnification of $30\times$ allows to observe a relatively large area of the microsection. The merging of separate images to a macro-image allows to observe the dendritic structure of the whole cross-section area.

The X-ray diffraction topography, used to analyse the defect structure, is based on differences in the intensity of X-ray reflected beam, registered from defected and non-defected fragments of the sample. A characteristic X-ray incident beam strikes the sample, which may oscillate simultaneously with the detector – X-ray film (Auleytner method) [13,14]. The PANalytical diffractometer, equipped with a copper microfocus source, emitting a divergent X-ray beam ($\lambda = 1.542 \text{ \AA}$) was used for the analysis. The X-ray film oscillation was $\pm 4^\circ$.

3. Results and Discussion

The dendritic structure of analysed blade roots is typical of CMSX-4 superalloy in the *as-cast* state (Fig. 3). However, it is not homogeneous in the whole volume of the blade roots. The dendrites are arranged in dendritic bands in most areas of the roots. These areas of high dendrites regularity are located around region S (Fig. 3) which is located above the place where the root is connected with a selector and hereinafter referred to as a selector extension. In the areas of root outside edges and areas of cooling bores (KW1, KW2, KW3 – Fig. 3) the dendritic structure is disordered. Characteristic types of structure disorders are indicated in Fig. 3 by dashed lines.

The most regular dendritic structure occurs in the area of selector extension along the main blade axis (area S – Fig. 3). Parallel bands of dendrites are arranged regularly, the dendrite arms are distributed symmetrically and possess a similar shape and size (Fig. 4). The inclination of dendrite bands in relation to the longer edge of the sample is approximately 49° .

The highest decrease in the quality of the structure was observed on the opposite side of the cooling bores, considering each metallographic section. The curvature of the dendrite bands shown in Fig. 5 is the example of disorders in this area (area 1 – Fig. 3). The arms of dendrites which grow directly from the selector are clearly greater than the arms on the other side of the visible curved band. In the area nearest to the band curvature, the dendrite arms are elongated, changing the orientation of the neighbouring bands.

Fig. 6 shows the dendritic structure in the area between cooling bores KW1 and KW2 (area 2 – Fig. 3). In this area, there are noticeable differences in the size of dendrite arms and changes in the interdendritic distance. The area closer to the cooling

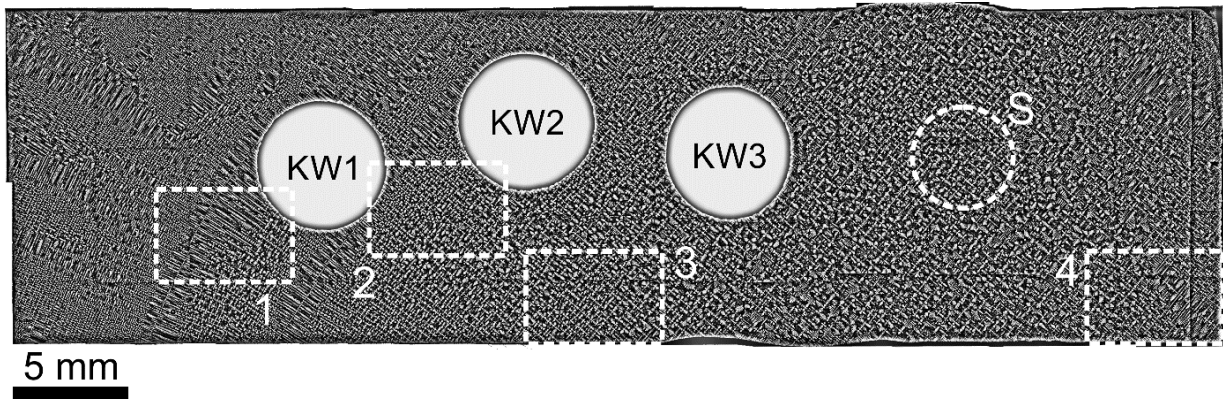


Fig. 3. Macro SEM image example (BSE technique) of the blade root dendritic structure

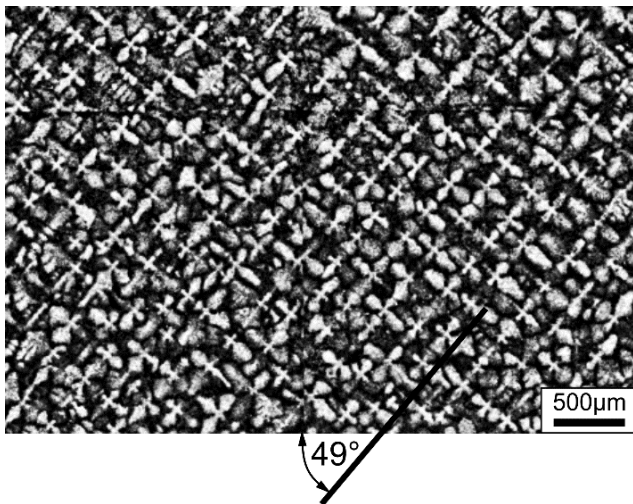


Fig. 4. Micro SEM image example (BSE technique) of the blade root dendritic structure in the area of selector extension along the main blade axis

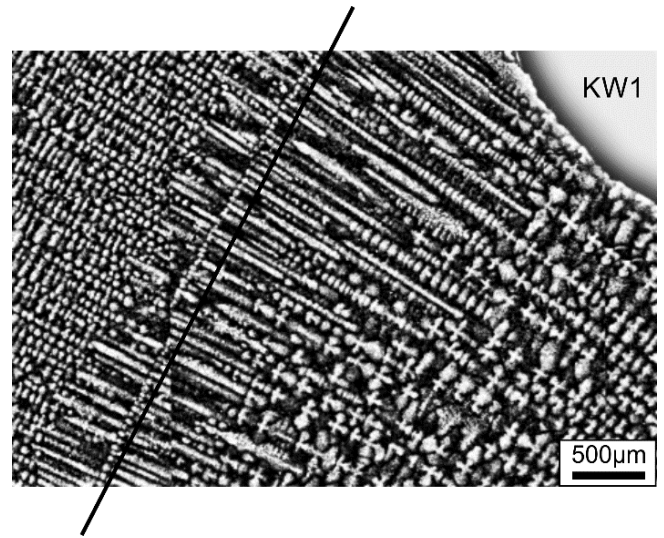


Fig. 5. SEM micrograph image (BSE technique) of the blade root dendritic structure in area 1 (Fig. 3)

bores and the region between them contain the finer dendrites structure with shorter dendrite arms. They are arranged in bands with a higher regularity as compared with an area distant from the cooling bores. Elongated dendrite arms (primary arms) can be observed in some fragments of the area around the cooling bores, for example, near the KW1 bore.

Similar changes occur in the area located on the edge of the blade root shown in Fig. 7. The area being closer to the edge (the bottom of Fig. 7) has a finer structure with dendrite arms smaller in size. The arms are often asymmetrical and have irregular shapes. Bands of dendrites, both smaller and larger in size, are often disturbed and discontinued.

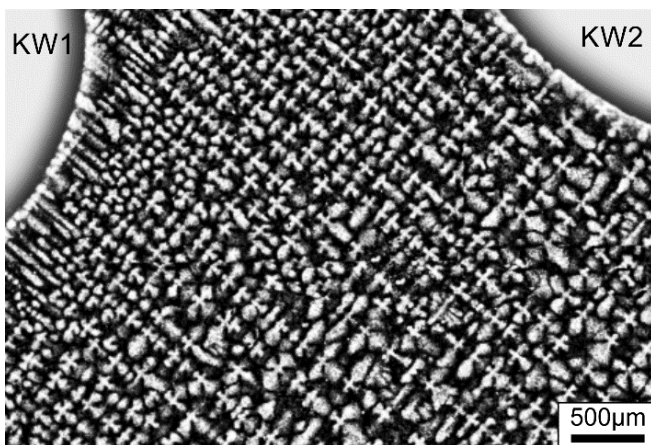


Fig. 6. SEM micrograph (BSE technique) of blade root dendritic structure in area 2 (Fig. 3)

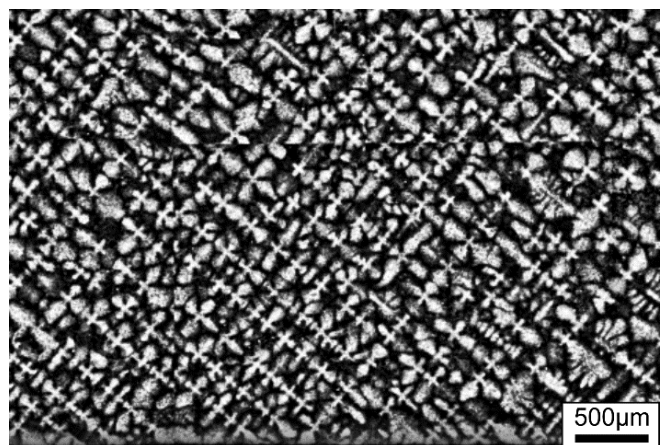


Fig. 7. SEM micrograph (BSE technique) of the blade root dendritic structure in area 3 (Fig. 3)

The fragment of microstructure shown in Fig. 8 and marked by an ellipsis is characterized by a very high elongation of dendrite arms (primary arms). They have a shape of long, thin rods. Additionally, in the areas of excessive growth of dendrite primary arms the growth of secondary arms is visible. Secondary dendrite arms have a needle-like shape and are densely arranged on the primary dendrite arms. This type of structure is often found near the corner areas of samples and in some areas around the cooling bores. When the distance from the edge of roots is higher, the dendritic structure is more ordered. The dendrite arms (primary arms) become more regular and the growth of secondary dendrite arms is blocked.



Fig. 8. SEM micrograph (BSE technique) of the blade root dendritic structure in area 4 (Fig. 3)

The crystallographic orientation analysis by the Laue method was performed in several selected areas on each sample: near the selector extension area, in the area between the cooling bores, near the edges and corners of the blade roots and in the area opposite to the selector side (in the section plane) relative to the cooling bores. An example of the Laue pattern obtained from an area located at a larger distance from the selector is shown in Fig. 9. Strongly blurred and inconsistent Laue spots are visible, which are arranged symmetrically, characteristic of the symmetry of a cubic crystal system. The central spot, created from (001) type planes, is displaced from the central hole. The Laue patterns received for areas closer to the selector area feature a higher spots consistency and proportionality. The spot representing the [001] direction coincides with the central hole.

X-ray diffraction topography studies were conducted for 002 and 113 reflections. The topograms for those reflections are subjected to geometric distortions, hence topograms do not mirror the shape of the tested samples. Topograms shown in Fig. 10 and Fig. 11 have different degrees of deformation due to different reflections and a different distortion level.

Fig. 10 shows a typical topogram, obtained for the analysed turbine blade roots for the 002 reflection. Parallel contrast bands are visible, extending along *k* and *l* lines. These bands are mutually perpendicular, when taking into account the correction for geo-

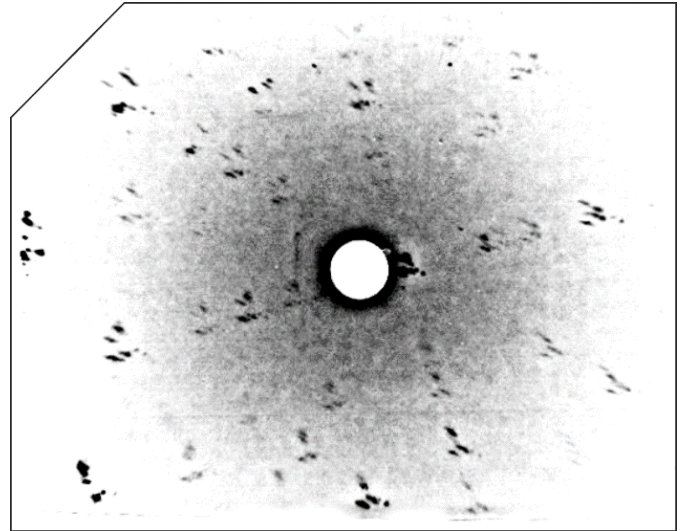


Fig. 9. Example of Laue pattern obtained from the area with high disorder in the dendritic structure; [001] direction

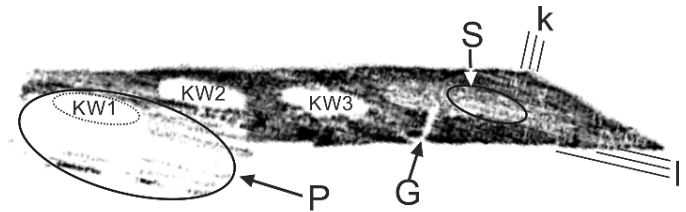


Fig. 10. Example of topogram obtained from blade root with X-ray film oscillation; 002 reflection, $\text{CuK}\alpha_1$ radiation

metric distortion of the topograms. It is mostly visible in the areas close to the selector extension (S area). An increased contrast is visible near the edges of the blade roots and between the cooling bores. Also a bright longitudinal region of missing contrast (G) can be seen, which extends from the edge of the topogram. Area P, indicated in Fig. 10 by a black oval, is located partially outside the main contour of the topogram. It is caused by a shift of a topogram fragment, which was created as a result of different diffraction conditions in a part of the represented sample. This area is characterized by parallel weak contrast bands with the same orientation as line *l*, but with a greater band distance.

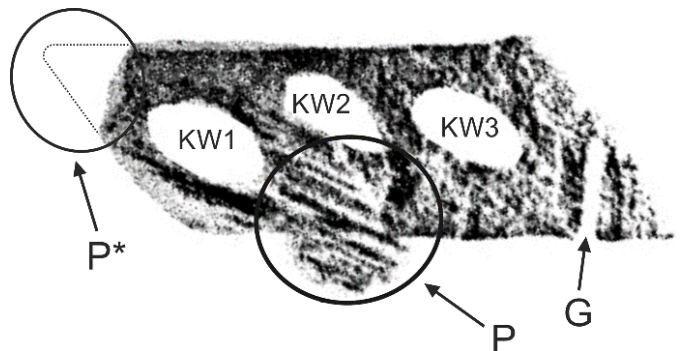


Fig. 11. Example of topogram obtained from the blade root with X-ray film oscillation; 113 reflection, $\text{CuK}\alpha_1$ radiation

Fig. 11 shows a typical topogram of analysed blade roots, obtained for the 113 reflection. The X-ray beam does not cover the entire sample surface, but the area of cooling bores. Parallel contrast bands are almost invisible in the topogram, except for area P, which overlaps the base image by shifting from the P* area. This shift and distortion is the result of different diffraction conditions in a part of the represented sample. The longitudinal area of the lacking contrast, starting from the edge of the sample and marked as G (Fig. 11), is also visible in the topogram.

The analysed cored blade roots have a dendritic structure, which is shown on SEM images of transverse sections (Fig. 3, Fig. 4). The dendritic structure of the areas of most samples is characterized by mutually orthogonal, intersecting bands of dendrite cores, visible on the micrographs in the form of crosses, distributed regularly along certain directions. The observed dendritic structure is regular and the dendrites are arranged evenly and linearly. This type of structure is found in the area near the selector, from which the direct growth of dendrites takes place during the solidification. This area is distant from the walls and cooling bores, so that they do not have significant influence on the dendrites growth. Some areas were observed, where the structure had a deviation from the typical one, occurring in the undisturbed areas of blade roots. Disturbances in the form of reduced distance between the dendritic arms, changes in the shape of dendrites and directions of dendritic bands, their curvature or total lack of order – occur most frequently in the areas close to the edge of the sample, between the edges and cooling bores and between the bores.

The contrast visible on topograms is obtained mainly from the γ' phase, which has the largest volume fraction in the analysed CMSX-4 superalloy. Parallel contrast bands correspond to ordered bands of dendrites, visible on the SEM images. An increased contrast shows a crystallographic misorientation in some areas, which is visible at the edges and especially in the corners of samples. The elongated narrow areas of the lack of contrast in topograms (G – Fig. 10 and Fig. 11) indicate a low angle boundary. The areas on the topogram, where the contrast is blurred or missing, correspond to the areas of structure disturbances shown on the SEM images.

The Laue method studies showed that some areas of the samples had a lower structural perfection and higher crystallites disorientation. It is confirmed by the distortion and blur and, in extreme cases, by the divergent nature of Laue spots in some Laue patterns. All results, that show structural defects in certain areas of the blade roots, were obtained from the same areas, but with the use of different methods. These results are mutually complementary. The Laue patterns indicating crystallite disorientation (Fig. 9) correlate with the areas in the topograms, where the lack of and a blurred contrast or shifts were visible (P, Fig. 10, Fig. 11) and the structure is disturbed in SEM images (Fig. 5).

4. Summary and conclusions

The *as-cast* single-crystalline cored blade roots made of CMSX-4 nickel superalloy were analysed. Blade roots have a dendritic structure, which is not homogenous in their entire volume. There are differences in the size of dendrite arms and in the interdendritic distance, most frequently depending on their location relative to the selector. These inhomogeneities of the structure may be caused by differences in the crystallization rate at the local areas. The structural perfection of the blade roots is greater in the area of the selector extension along the main axis of the blade. A decrease of the microstructure quality at the increasing distance (in a plane perpendicular to the blade axis) from the selector extension along the main axis is caused by the occurrence of low-angle boundaries and other structural defects, formed during the crystallization. Also the growth of dendrites in certain directions is limited and distorted by the presence of cooling bores. In the blades casting process the ‘inheritance’ of defects in the dendrite arms’ growth occurs. When a growing dendrite meets the barrier of cooling bores or the crucible wall, the direction of growth may be changed, causing disturbance to the structure during further growth.

It is probably possible to select the optimal parameters of the crystallization process and the geometric distribution of cooling bores in a blade volume, for which the number of processes of ‘inheriting’ structure disturbances will be the lowest. In this case, the size and distribution of the cooling bores must be precisely determined, as well as the size and geometry of the blade roots. A smaller cooling bores diameter may reduce their influence on the creation of subgrains and other structural defects.

Acknowledgments

The author would like to thank the management and employees of the Department of Materials Science and Research & Development Laboratory for Aerospace Materials, Rzeszów University of Technology for the cooperation and valuable help.

REFERENCES

- [1] R.C. Reed, *The Superalloys, Fundamentals and Applications*, Cambridge University Press, Cambridge 2006.
- [2] J.C. Williams, E.A. Strake, *Acta Mater.* **51**, 5775 (2003).
- [3] M.J. Donachie, S.J. Donachie, *Superalloys, a Technical Guide*, ASM International, Ohio 2002.
- [4] W. Betteridge, S.W.S. Shaw, *Development of superalloys*, *J. Mater. Sci. Technol.* **3**, 682 (1987).
- [5] J-Ch. Han, S. Dutta, S. Ekkad, *Heat transfer and cooling technology*, CRC Press, Boca Raton, USA (2013).

- [6] A. Onyszko, W. Bogdanowicz, J. Sieniawski, *Solid State Phenom.* **186**, 151 (2012).
- [7] E. Sun, T. Heffernan, R. Helmink, *Stress rupture and fatigue in thin wall single crystal superalloys with cooling holes in: Superalloys 2012*, Eric S. Huron (Ed.), TMS, Willey (2012).
- [8] A. Onyszko, J. Sieniawski, W. Bogdanowicz, H. Berger, *Solid State Phenom.* **177**, 203-204 (2013).
- [9] B. Dubiel, *Zmiany mikrostruktury podczas pełzania monokrystalicznych nadstopów niklu*, Wydawnictwa AGH, Kraków 2011.
- [10] C. Walter, B. Hallstedt, N. Warnken, *Mat. Sci. Eng. A-Struct.* **397**, 385 (2005).
- [11] M. Durand-Charre, *The Microstructure of Superalloys*, CRC Press, London 1997
- [12] Z. Trzaska Durski, H. Trzaska Durska, *Podstawy krystalografii strukturalnej i rentgenowskiej*, PWN Warszawa 1994.
- [13] J. Auleytner, *Acta Phys. Pol. A* **17**, 111 (1958).
- [14] W. Bogdanowicz, *Scripta Mater.* **31**(6), 829 (1997).